Recognition of Upper Airway and Surrounding Structures at MRI in Pediatric PCOS and OSAS

Yubing Tong[1], J.K.Udupa[1], D Odhner[1], Sanghun Sin[2], R Arens[2]
[1]Medical Image Processing Group, Dept. of Radiology, University of Pennsylvania, 423 Guardian Drive, Blockley Hall, 4th Floor, Philadelphia, PA 19104
[2]The Children's Hospital at Montefiore, Albert Einstein College of Medicine, Bronx, NY.

ABSTRACT

Obstructive Sleep Apnea Syndrome (OSAS) is common in obese children with risk being 4.5 fold compared to normal control subjects. Polycystic Ovary Syndrome (PCOS) has recently been shown to be associated with OSAS that may further lead to significant cardiovascular and neuro-cognitive deficits. We are investigating image-based biomarkers to understand the architectural and dynamic changes in the upper airway and the surrounding hard and soft tissue structures via MRI in obese teenage children to study OSAS. At the previous SPIE conferences, we presented methods underlying Fuzzy Object Models (FOMs) for Automatic Anatomy Recognition (AAR) based on CT images of the thorax and the abdomen. The purpose of this paper is to demonstrate that the AAR approach is applicable to a different body region and image modality combination, namely in the study of upper airway structures via MRI.

FOMs were built hierarchically, the smaller sub-objects forming the offspring of larger parent objects. FOMs encode the uncertainty and variability present in the form and relationships among the objects over a study population. Totally 11 basic objects (17 including composite) were modeled. Automatic recognition for the best pose of FOMs in a given image was implemented by using four methods – a one-shot method that does not require search, another three searching methods that include Fisher Linear Discriminate (FLD), a b-scale energy optimization strategy, and optimum threshold recognition method. In all, 30 multi-fold cross validation experiments based on 15 patient MRI data sets were carried out to assess the accuracy of recognition. The results indicate that the objects can be recognized with an average location error of less than 5 mm or 2-3 voxels. Then the iterative relative fuzzy connectedness (IRFC) algorithm was adopted for delineation of the target organs based on the recognized results. The delineation results showed an overall FP and TP volume fraction of 0.02 and 0.93.

Keywords: Segmentation, Object Recognition, Fuzzy models, Obstructive sleep apnea, Fuzzy connectedness.

1. INTRODUCTION

Polycystic Ovary Syndrome (PCOS) is one of the most common disorders associated with overweight and obesity and it affects 5-10% of adolescent girls and women of reproductive age. Obstructive Sleep Apnea Syndrome (OSAS) is common in obese children with risk being 4.5 fold compared to normal control subjects. PCOS has recently been shown to be associated with OSAS that may further lead to significant cardiovascular and metabolic derangements in these subjects [1]. We are investigating image-based biomarkers to understand the pathophysiological mechanisms leading to OSAS in adolescent girls with PCOS by studying the architectural and dynamic changes in the upper airway and surrounding skeletal and soft tissues via MRI. Manual or human assisted segmentation was previously used for the quantification of upper airway and surrounding structures at MRI [1]. For large-scale population studies, and in studies involving dynamic images, this becomes a hindrance. Computerized automatic anatomy recognition (AAR) may be helpful in such situations [2, 3]. The goal of AAR is to identify and delineate the various organs in a body region automatically in a given patient image of the body region.

We previously presented a methodology for AAR based on Fuzzy Object Models (FOMs). We pursued the development of fuzzy anatomy modeling principles to find natural and computationally efficient means of bringing anatomic knowledge about large assemblies of objects into graph-based approaches such as fuzzy connectedness [4]. The hierarchical arrangement inherent in the anatomic layout of organs was modeled to make AAR effective and efficient. The purpose of this paper is to demonstrate the use of FOMs in performing AAR of upper airway structures. The AAR approach consists of three main steps: (a) model generation from image data; (b) object recognition in a given image

Medical Imaging 2013: Computer-Aided Diagnosis, edited by Carol L. Novak, Stephen Aylward, Proc. of SPIE
Vol. 8670, 86702S · © 2013 SPIE · CCC code: 1605-7422/13/$18 · doi: 10.1117/12.2007948

using the models; (c) delineation and quantification of the recognized objects. Given the premise of this paper, the focus here is on (b) and (c) for upper airway system and surrounding structure segmentation.

The paper is organized as follows. The AAR method is described in Section 2, which includes fuzzy object modeling, recognition as well as delineation. Recognition and delineation results are shown in Section 3 with quantitative and qualitative evaluation. Conclusions are given in Section 4.

2. ADAPTATION OF THE AAR METHOD TO THE UPPER AIRWAY REGION

The AAR approach consists of three steps as shown in Figure 1. First, the objects in the body region to be included in the model for the body region are determined and a hierarchy for their arrangement is determined. For each object, such as the mandible, its samples from different subjects are used for building fuzzy object (mandible) model. Such models for all objects together with the learned hierarchical relationship constitute a fuzzy model of the body region. Then this model assembly is used in the recognition step to find out where each target organ is in a given image following the hierarchical order. Then in the delineation step, the organ boundary is segmented. This paper mainly focuses on recognition and delineation as applicable to the upper airway organ system (UAOS). FOMs for 17 objects in UAOS are arranged in a hierarchical order as in Figure 2. The objects included are: skin boundary (body region outline), airways and bone (as a composite object), soft tissues (as a composite object), pharynx (nasopharynx and oropharynx), fat pad, mandible, oropharynx, tonsils (left and right), adenoid, soft-palate, and tongue. FOMs encode the uncertainty and variability present in the position, size, and orientation of and the relationships among the various objects over the population.

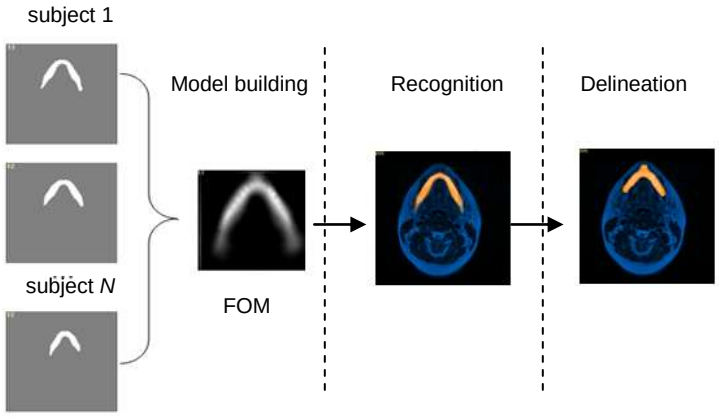

Figure 1. AAR framework showing the three steps: building FOMs, recognition, and delineation.

2.1 Fuzzy models

Given input images $I_1,\ldots, I_N$ for the UAOS body region B for N subjects, and segmentations of objects $O_1,\ldots, O_L$ of B in $I_1,\ldots, I_N$, the fuzzy object model of B is described as $FOM(B) = (H, M, FM, \rho, \eta)$. Here, H is a hierarchy of organs in B, expressed as a tree as in Figure 2. $M = \{FM_\ell : 1 \le \ell \le L\}$ is a set of fuzzy models, each FM_ℓ representing one of L organs as a fuzzy set over N subjects. ρ denotes the parent-to-offspring relationship in H over N subjects. λ is a set of scale factor ranges $\{\lambda_\ell : 1 \le \ell \le L\}$, λ_ℓ being a scale factor range for organ O_ℓ over N subjects. η is a host of measurements pertaining to organs in B. Further details on the model building step can be found in [3].

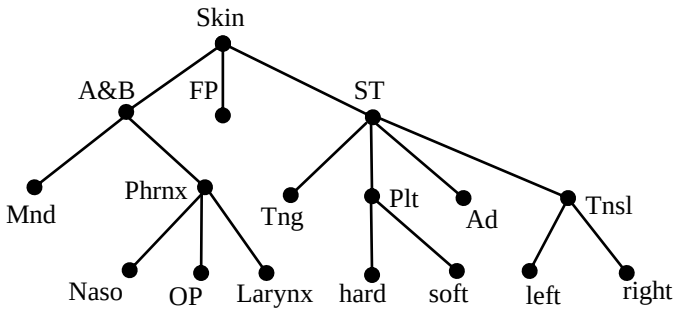

Figure2. Hierarchical representation of the upper airway organ system. A&B: airways and bone; FP: fat pad; ST: soft tissues; Mnd: mandible; Phrnx: pharynx including naso-pharynx, oro-pharynx (OP) and larynx; Tng: tongue; Plt: palate including hard and soft palate (SP); Ad: Adenoid; Tnsl: tonsils.

2.2 Recognition in AAR

We break up the AAR task for a given image *I* into recognition and delineation. The goal of recognition is to determine the objects' whereabouts in the image and the goal of delineation is to determine their spatial extent in the image and to mark the precise spatial occupation in *I*. The two components are interdependent and operate in tandem. Four recognition methods were tested.

Given *FOM*(*B*) and a new test image *I*, the recognition method will determine the 'best' pose (location, orientation, and scale factor) for the object's model for each object in image *I* so the models fall in place as closely as possible to the actual organ manifestation in *I*. Two kinds of recognition methods were studied. The first involves searching with 3 different searching strategies and the second involves no searching.

Search based approaches: To determine the optimum pose for object O_k, a subset of the search space is determined based on variations observed in $\rho_{l,k}$ and λ_k. This subspace is then sampled at regular discrete intervals, and at each sample pose, a "recognition score" is valuated to examine the degree of match of FM_k with the evidence available in *I* for O_k. The pose returning the maximum score is considered to be the pose recognizing object O_k. We have explored Fisher Linear Discriminate (FLD), minimizing ball-scale-based (b-scale) energy, and optimum threshold for searching for the best pose.

For the FLD method, the recognition score is based on the best separating FLD plane, which is derived from FLD feature classifier. Let *u* be the normal vector to the FLD plane derived from training and S'_k be the set of feature vectors *v* sampled on the model at pose *p*. Then the recognition score at pose *p* is taken to be $F_u(p) = (\sum_{v \in S'_k} v) \bullet u$.

For b-scale method, the energy function associated with FM_k at pose *p* in *I* is $E(p) = \sum_{c \in Q_p} f_b(c)$, where $f_b(c)$ is ball scale value of *I* at voxel *c*, and Q_p is the set of voxels corresponding to pose *p* of FM_k at which the model membership is about 0.5; more details about ball scale transform can be found in [6].

For the optimum threshold method, given a specific organ O_k, we can fix the corresponding threshold interval TH_k (optimum threshold) for it by checking all the training images. Then with that threshold, we segment the test image *I* roughly which will include a good portion of the target organ although there may be some other neighboring organs or tissues but the organs outside this intensity threshold interval will not disturb our recognition process. The optimal pose is the one for which we get the minimum difference between modified model and the threshold result.

One-shot method: The pose of the model in *I* is determined from the pose of the root object (skin boundary) and $\rho_{l,k}$. The root object is recognized and delineated by thresholding and searching for optimum fit with the model.

2.3 Delineation

A delineation method is used to precisely describe the target organ after we have found where the target organ is in the test image by the recognition process. We have explored the fuzzy connectedness family of algorithms including the basic fuzzy connectedness algorithm and iterative relative fuzzy connectedness (IRFC) as well as graph cut in our previous research [4, 5]. We have also proved seed robustness for fuzzy connectedness compared to graph cut which means that for FC or IRFC, we need only a few effective seed samples. Seeds are selected automatically by thresholding the fuzzy object model and the image simultaneously. The IRFC algorithm is used subsequently with a modification to take into account in addition to the image homogeneity and object feature components of affinity also a model based component.

3. RESULTS

Image data: T2-weighted MR images with voxel size 0.5 x 0.5 x 3.3 mm^3 from 15 control subjects (age from 8 to 17) were utilized in our experiments. Both axial and sagittal images were available. Some objects were delineated on axial images and others on sagittal. This posed some problems for model building and recognition. We carried out multiple recognition experiments (30 in all) with the "leave-4-out" strategy by randomly selecting 11 data sets for building the model and the remaining 4 for testing recognition performance and by changing this selection each time. The delineations of the objects required for model building were created by manual segmentation. Figure 3 shows some of the objects in the UAOS used in model building, and Figure 4 shows some sample fuzzy object models created from the training object samples.

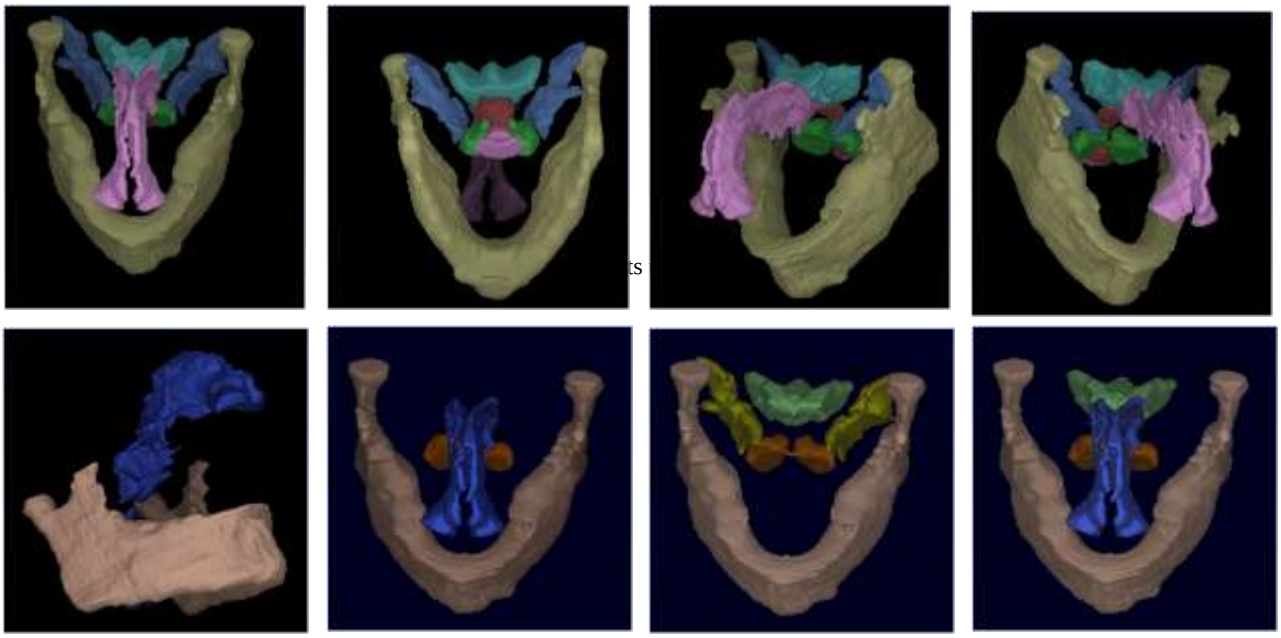

Figure 3. 3D surface renditions of sample objects used in model building.

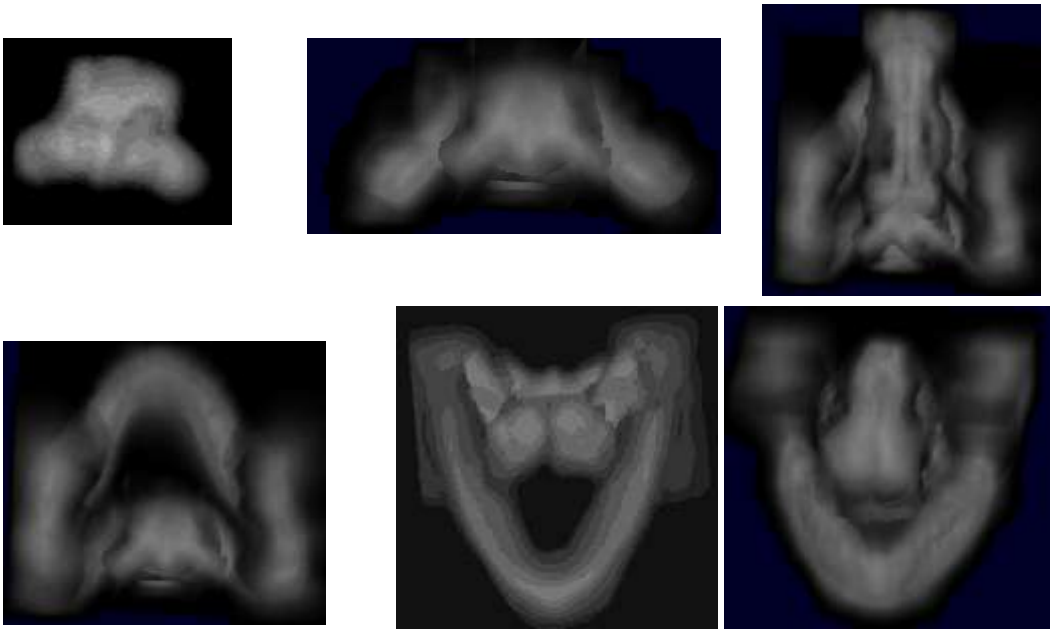

Figure 4. Sample fuzzy models shown in volume rendering.

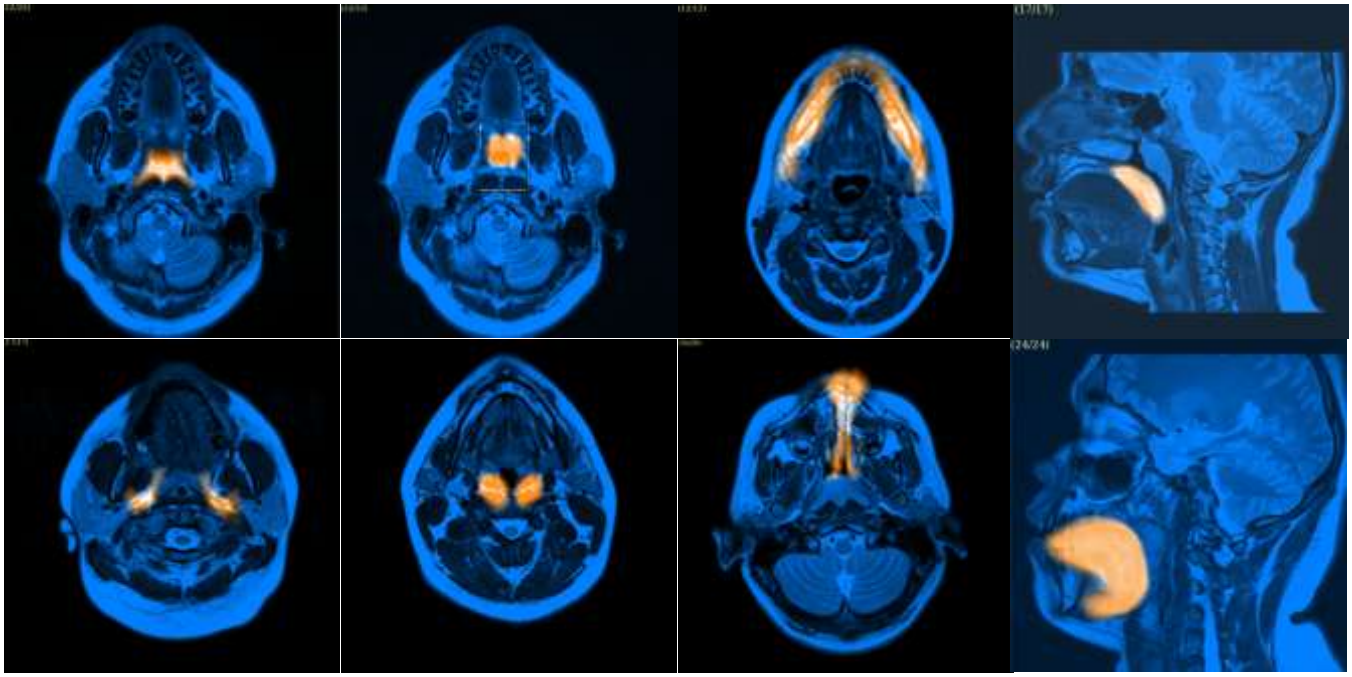

Figure 5. Sample recognition results with the model at recognition overlaid on the test image slices. The models appear as a bright orange cloud over slice display. L to R, top to bottom: Ad, OP, Mnd, SP, FP, Tnsl, Phrnx, and Tng.

Figure 5 displays recognition results, with models resulting from recognition overlaid on the original images. Table 1 lists the recognition results for all methods showing the errors in location and scale factor estimation. The mean and standard deviation over the 30 experiments are listed for each object. The location error is in mm. The scale factor error is expressed as a ratio of the estimated scale factor to the true scale factor (the ideal value thus being 1). Fuzzy object model building requires about 10 minutes per object, which can be done off-line. Once the model is built, recognition

takes less than 8 seconds per object for one-shot method and about 1 minute for the optimum-threshold method. Other methods take about 2 minutes per object.

Table 1. Recognition results for the FLD, one-shot, b-scale, and optimum threshold methods with average location error (Loc err. mean) and its standard deviation (std) and scale error (Scale err. mean) and its standard deviation (std). The objects listed are: Skin, Air & Bone (A&B), Soft-Tissue (ST), Pharynx, fat pad (FP), Tonsils (Tnsl), Adenoid (Ad), Oropharynx (OP), mandible (Mnd), soft-palate (SP), and tongue (Tng).

Method	Error	Skin	A&B	ST	Phrnx	FP	Tnsl	Ad	OP	Mnd	SP	Tng	Mean
FLD	Loc err. Mean	8.66	10.46	9.43	7.99	8.95	8.04	7.68	9.38	10.40	7.88	9.16	8.92
	std	4.53	3.52	5.68	2.94	4.07	5.13	4.64	4.95	3.67	4.54	3.73	4.31
	Scale err. mean	0.98	0.99	1.00	0.98	0.97	0.98	0.98	0.91	0.98	0.94	1.02	0.98
	std	0.02	0.05	0.05	0.06	0.06	0.17	0.11	0.12	0.05	0.18	0.07	0.09
One-shot	Loc err. mean	9.38	13.86	14.84	11.34	11.39	14.35	13.81	12.66	14.34	11.77	12.95	12.79
	std	4.41	4.15	5.37	4.01	4.01	4.27	4.62	5.59	3.87	4.72	4.15	4.47
	Scale err. mean	1.00	1.01	1.02	1.01	0.99	1.01	1.02	0.95	1.01	0.98	1.02	1.01
	std	0.01	0.05	0.05	0.07	0.06	0.16	0.11	0.11	0.06	0.13	0.06	0.08
B-scale	Loc err. mean	8.49	12.29	13.23	10.78	10.32	12.69	12.13	13.41	14.99	10.64	12.26	11.93
	std	4.60	3.33	4.77	3.41	4.21	4.02	3.73	4.57	4.55	5.34	4.62	4.28
	Scale err. mean	0.97	0.98	0.98	0.97	0.96	0.98	0.98	0.94	0.98	0.89	0.99	0.97
	std	0.02	0.06	0.05	0.06	0.05	0.16	0.11	0.10	0.05	0.16	0.06	0.08
Optimum threshold	Loc err. mean	1.80	2.77	4.94	7.38	2.53	1.93	2.16	3.85	8.92	5.17	5.12	4.23
	std	1.31	0.81	2.12	1.85	1.44	0.99	0.85	3.63	0.87	4.09	2.86	1.89
	Scale err. mean	1.01	0.98	0.99	1.04	0.99	0.97	1.01	1.11	0.95	1.04	1.01	1.01
	std	0.00	0.05	0.01	0.06	0.04	0.13	0.13	0.15	0.06	0.15	0.14	0.04

Delineation results are shown in Figure 6 and Table 2. In Figure 6, the IRFC results are overlaid on the test image slices. 3DVIEWNIX and CAVASS software were used for processing and visualization [7].

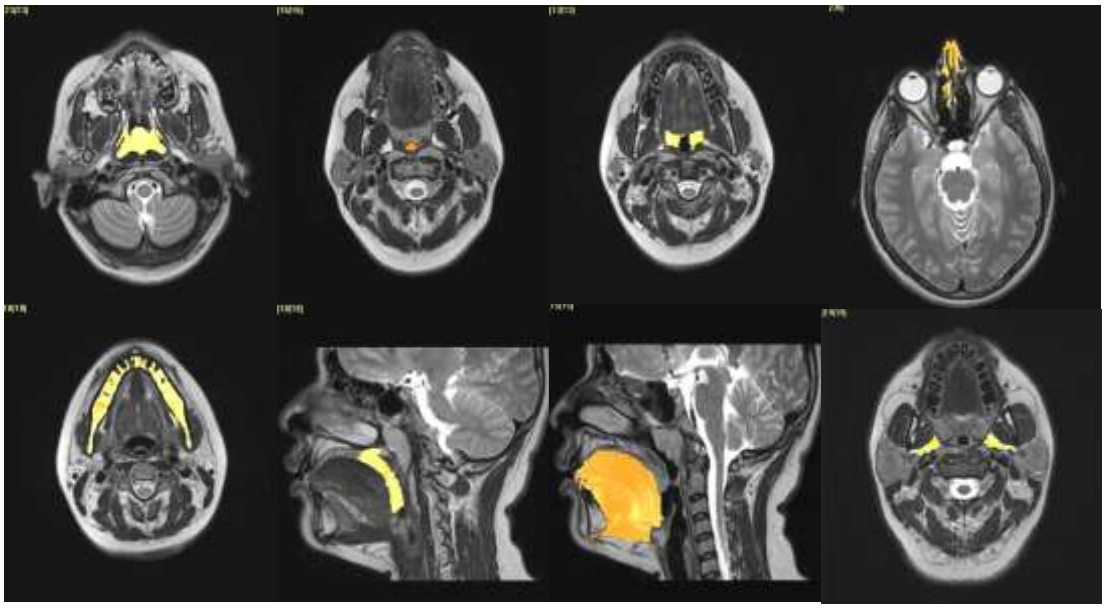

Figure 6. IRFC Delineation results. The bright orange overlays correspond to the delineated region. Objects shown are: Ad, OP, Tnsl, Phrnx (nasal), Mnd, SP, Tng, and FP.

Table 2. Delineation results from IRFC. TPVF and FPVF: True positive and false positive volume fractions [8].

	Skin	A&B	ST	Mnd	Phrnx	OP	FP	Ad	Tnsl	Tng	SP
TPVF	0.91	0.90	0.96	0.34	0.93	0.91	0.93	0.97	0.96	0.87	0.53
FPVF	0.02	0.10	0.01	0.01	0.03	0.00	0.00	0.00	0.00	0.01	0.01

4. CONCLUDING REMARKS

In the original FOM method, the body regions of focus were the thorax and abdomen based on contrast-enhanced CT images. We demonstrate in this paper that the exact same approach and software is applicable to a different body region and image modality for applications in PCOS and OSAS.

Fuzzy object modeling is feasible for the upper airway region. The AAR results obtained for this body region seem to be superior to the results originally obtained for the thorax and abdomen in absolute measures. One of the reasons may be the smaller voxel size in these images of the neck region. The AAR method is effective in different body regions under different modalities calling for little change to the software.

The optimum-threshold method achieved the best recognition results (within about 2 voxels of the true locations, scale factor estimation being uniformly excellent), for some objects substantially better than the other three methods. In all our experiments, we have ignored orientation, in both model building and recognition search. Orientation adjustment may further improve the results although this will make the computations more expensive.

Delineation via the IRFC method could effectively segment most of the target organs except a couple of organs like mandible and soft palate. The delineation results showed an overall FP and TP volume fraction of 0.02 and 0.93 except those two organs, which is generally considered to be excellent.

In the study of OSAS, the dynamics of the airway structure becomes an important factor. We have started gathering dynamic MR images of the study subjects and extending the FOM principles to dynamic fuzzy models.

Acknowledgments

This research is supported by a DHHS grant HL 105212.

REFERENCES

[1] Arens R., Sin S., Nandalike K., Rieder R., Khan UI., Freeman K., Wylie-Rosett J., Lipton ML., Wootton DM., McDough JM., Shifteh K., "Upper Airway Structure and Body Fat Composition in Obese Children with Obstructive Sleep Apnea Syndrome, " American Journal of Respiratory and Critical Care Medicine 183, 782-787 (2011).

[2] Udupa, J.K., Odhner, D., Falcao, A.X., Ciesielski, K.C., Miranda, P.A.V., Matsumoto M., Grevea, G.J., Saboury, B., and Torigian, D.A., "Automatic Anatomy Recognition via Fuzzy Object Models," Proc. SPIE 8316, 5-8 (2012).

[3] Udupa, J.K., Odhner, D., Falcao, A.X., Ciesielski, K.C., Miranda, P.A.V., Matsumoto M., Grevea, G.J., Saboury, B., and Torigian, D.A., "Fuzzy object modeling," Proc. SPIE 7964, 1-10 (2011).

[4] Ciesielski, K.C,. and Udupa, J.K., Falcao, A.X., Miranda, P.A.V., " Comparison of fuzzy connectedness and graph cut segmentation algorithms," Proc. SPIE 7962, 3-10 (2011).

[5] Chen, X., Udupa, J.K., Alavi, A., and Torigian, D.A., "Automatic anatomy recognition via multiple object oriented active shape models, " Medical Physics 37, 6391-6401 (2010).

[6] Saha, P. and Udupa, J.K., " Scale-based fuzzy connected image segmentation: Theory, algorithm and validation," Computer Vision and Image Understanding, 77(2):145-174 (2000).

[7] Grevera, G., Udupa, J.K., Odhner, D., "CAVASS: a framework for medical imaging applications," Proc. SPIE 7497, MIPPR 2009.

[8] Udupa, J.K., LeBlancb, V.R., Imielinskab, C., Currief, L. M., Hirschg, B. E., Woodburnh, J., "A framework for evaluating image segmentation algorithms," Computerized Medical Imaging and Graphics, 30, 75-87 (2006).